Diagnosis of suspected hypovitaminosis A using magnetic resonance imaging in African lions (*Panthera leo*)

M P Hartley[a*], R M Kirberger[b], M Haagenson[c] and L Sweers[b]

ABSTRACT

Vitamin A deficiency is described in captive lions. *Ante mortem* diagnosis can either be made by serum analysis or liver biopsy, both of which may be problematic. This study utilised magnetic resonance imaging to identify vitamin A deficiency in lions with relatively mild clinical signs, which could otherwise be attributed to numerous other neurological conditions. Magnetic resonance imaging is a non-invasive, reliable diagnostic tool to demonstrate pathology typically associated with this condition. To accommodate varying lion ages and sizes, a number of cranium and brain measurements were compared with that of the maximum diameter of the occular vitreous humor. Occular ratios of the *tentorium cerebelli osseum* and occipital bone were most reliable in diagnosing the thickened osseous structures characteristic of hypovitaminosis A. The ratio of maximum:minimum dorsoventral diameter of the C1 spinal cord was also of value.

Key words: hypovitaminosis A, magnetic resonance imaging. *Panthera leo.*

Hartley M P, Kirberger R M, Haagenson M, Sweers L **Diagnosis of hypovitaminosis A using magnetic resonance imaging in African lions (*Panthera leo*)**. *Journal of the South African Veterinary Association* (2005) 76(3): 132–137 (En.). The World Owl Trust, Muncaster Castle, Ravenglass, Cumbria, UK.

INTRODUCTION

Hypovitaminosis A occurs occasionally in captive lions (*Panthera leo)* where it is associated with exclusive feeding of lean red meat[2,6]. Clinical signs include incoordination, 'star-gazing', ataxia, apparent blindness, circling and nystagmus progressing to convulsions. Death may result approximately 2 months after the onset of clinical signs[2]. The clinical signs are caused by severe thickening of the cranial bones with consequential compression of the brain and eventual prolapse of the cerebellum through the foramen magnum[2,6]. Cervical vertebrae may also be thickened resulting in compression of the cranial cervical spinal cord[6]. Diagnosis of hypovitaminosis A has traditionally been made by analysis of circulating blood levels, which is usually prohibitively expensive; or by liver biopsy, which carries a risk of haemorrhage. The use of imaging techniques to diagnose hypovitaminosis A have not been described to date. This paper describes the value of magnetic resonance imaging (MRI) as a diagnostic tool.

[a]The World Owl Trust, Muncaster Castle, Ravenglass, Cumbria, United Kingdom.

[b]Diagnostic Imaging Section, Department of Companion Animal Clinical Studies, Faculty of Veterinary Science, University of Pretoria, Private Bag X04, Onderstepoort, 0110 South Africa.

[c]Milpark Hospital, Guild Road, Parktown West, 2193 South Africa.

*Author for correspondence.
E-mail: mhzoovet@yahoo.com

Received: March 2005. Accepted: August 2005.

MATERIALS AND METHODS

Four clinically affected lion cubs (Cubs A, B, C and D), 3 white and 1 brown, aged between 6 and 9 months and weighing 20–46 kg were investigated over a period of 18 months. Cubs A and B were female litter mates and Cub C was a male with the same father but with a different mother, all from the Johannesburg Zoological Gardens. Cub D was a male from a farm in the Eastern Cape. All cubs were fed beef, horse or kangaroo meat on the bone but no offal**.** The clinical signs were noted, after which cubs A–C were anaesthetised by dart with 1 mg (0.05 mg/kg) medetomidine (Domitor, Novartis Animal Health) and 100 mg (5 mg/kg) ketamine (Ketamine Dry Powder, Kyron Laboratories). This was followed by a physical examination and a limited neurological examination. Blood was collected from the cephalic vein for routine haematology and biochemistry analysis. Serum was tested for canine distemper virus IgG and IgM antibodies as well as for feline leukaemia virus, feline immunodeficiency virus, feline corona virus, feline calici virus and feline panleukopaenia virus antibodies. A cerebrospinal fluid sample (CSF) was taken from Cub A for cytological evaluation.

Three days later each cub was again anaesthetised using the same protocol and MRI was performed with a Phillips Gyroscan T10 1.5 Tesla unit (Phillips Medical Systems). Sagittal, transverse and dorsal slices of the brain and upper cervical region were made using T1- and T2-weighted spin echo and fluid attenuating inversion recovery (FLAIR) sequences. Multiple 3–5 mm slices with 0.3–2 mm slice intervals were obtained. Cubs B and C also had specific transverse images made of the cochlear and vestibular apparatus. Additional T1-weighted images were made after intravenous administration of gadoteric acid paramagnetic contrast agent at 0.1 mmol/kg (Dotarem, AXIM). Six months following initial presentation, Cub A had a repeat MRI examination using the same protocol.

Cub D was clinically evaluated and then anaesthetised with midazolam (Hexal, Pharma SA) at 0.3 mg/kg and 70 mg ketamine (Ketamine Dry Powder, Kyron Laboratories) intramuscularly, followed by a propofol (Propofol 1 % Fresenius, Fresenius Kabi) infusion. Blood was collected for routine haematology and biochemistry analysis, including bile acids. Serum was tested for feline leukaemia virus, feline immunodeficiency virus and feline corona virus antibodies. Under the same anaesthesia MRI was performed with a General Electric Sigma 1.5 Tesla unit (General Electric Company). Similar slices and sequences to Cubs A–C were made in sagittal and transverse planes, including images of the inner ear. Gadodiamide paramagnetic contrast agent (Omniscan, Amersham Health) was given intravenously at 0.1 mmol/kg followed by sagittal and transverse T1-weighted images.

An unrelated 9-month-old apparently healthy lion (Cub E), which was not showing any of the clinical signs described, underwent a similar MRI examination using the same anaesthetic and imaging protocols as cubs A–C to act as a control.

Direct measurements were made on the laser printed MRI films using a vernier calliper and distances corrected for by using the cm scale present on each film. Measurements were made on the T1- and T2-weighted images by 2 authors (RK and LS) and averaged. The best images were

selected to make the measurements except for the spinal cord measurements, which were only made on T2-weighted images because the hyperintense CSF signal provided good contrast. The following measurements were made on various sagittal images: 1) the thickest part of the tentorium *cerebelli osseum* to the left and right of the midline; 2) the thickness of the parietal bone 10 mm caudal to the caudoventral aspect of the frontoparietal suture on midline images (Fig. 1); 3) the maximum thickness of the caudal basisphenoid bone on midline images (Fig. 1); 4) the horizontal thickness of the occipital bone 10 mm from its ventral extremity on midline images (Fig. 1); 5) the minimum and 6) maximum dorsoventral spinal cord diameters from cranial C1 to mid C2 on midline images (Fig. 1); 7) the maximum diameter of the vitreous humor of the eye caudal to the lens.

The following measurements were made on transverse images: 1) the thickest part of the *tentorium cerebelli osseum* to the left and right of the midline (Fig. 2); 2) the maximum midline thickness of the caudal basisphenoid bone; 3) the maximum dorsoventral distance of the cerebellum and associated brainstem added to the maximum latero-lateral diameter of the cerebellum at the level where the typanic bullae were at their largest; 4) the dorsoventral diameter of the lateral ventricles (left and right) 10 mm from the midline at the level of the interthalamic adhesion or hypophysis (Fig. 3) and 5) the midline cerebrum dorsoventral diameter including the *falx cerebri* (Fig. 3).

Owing to limited numbers, statistical analysis could not be performed. The maximum vitreous humor diameter was used to act as a reference measurement for comparative ratios of various structures to accommodate the different ages and weights of the cubs. Additionally the maximum and minimum dorsoventral cervical spinal cord diameters were compared as well as the height of the lateral ventricles *versus* the midline cerebrum height. All the ratios for the 4 affected cubs (excluding Cub A follow up) were averaged and compared to the normal cub to look for trends.

RESULTS

Cub A presented with a mild left-sided head tilt and intermittent circling behaviour. The cub was treated with clavulanate amoxycillin (Synulox 250, Pfizer Animal Health) and meloxicam (Metacam Oral Suspension, Boehringer Ingelheim). Clinical signs progressed over the next 3 days, with additional nystagmus and 'star-gazing' developing, after which MRI was performed. Cubs B & C had less

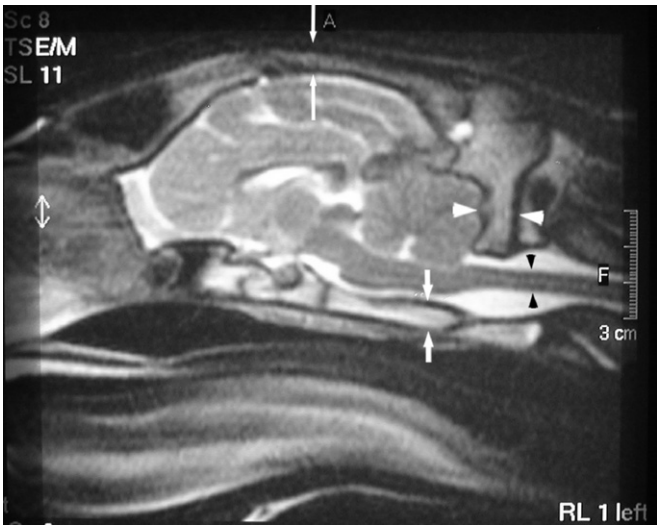

Fig. 1: **Sagittal midline T2 weighted brain image of normal Cub E. Measurement are indicated for the parietal bone** (long white arrows)**, basisphenoid bone** (short white arrows)**, occipital bone** (white arrow heads) **and spinal cord** (black arrow heads)**. Ignore white double arrowhead on left of image.**

Fig. 2: **Transverse T2 weighted brain image of normal Cub E at the level of the *tentorium cerebelli osseum.* Arrows indicate the thickest part of the bone to the left and right of the midline.**

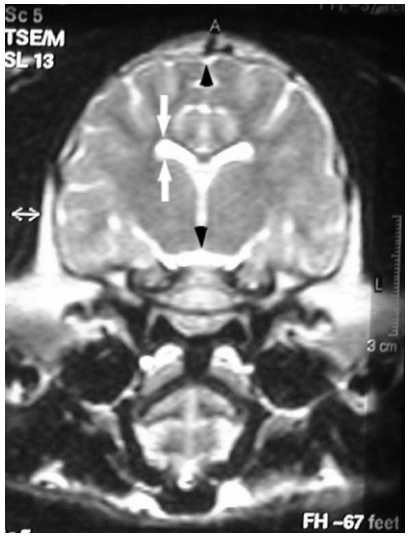

Fig. 3: **Transverse T2 weighted brain image of normal Cub E at the level of the 3rd ventricle/interthalamic adhesion area. White arrows indicate the dorsoventral diameter of the lateral ventricles. Black arrowheads indicate the midline cerebrum dorsoventral diameter. Lateral ventricle:cerebral ratio was 0.10. Ignore white double arrowhead on left of image.**

severe clinical signs with the one developing a mild head tilt and the other an intermittent circling behaviour. Cub D presented initially with an unsteady gait. This progressed over the next 2 months to a moderate head tilt and circling to the left with apparent blindness. There were no abnormal findings detectable in the blood or CSF.

Abnormal MRI findings in Cubs A–D included varying degrees of lateral ventricle dilation (Fig. 4) with poor visibility of the septum pellucidum in Cub A. The cortical and cerebellar sulci were generally effaced with poor CSF signal. The 3rd and 4th ventricles were compressed to varying degrees. The caudal fossae appeared small with the cerebellum being compressed from dorsally and caudally by a prominent *tentorium cerebelli osseum* and occipital bone respectively (Figs 5–7). Mild herniation of the cerebellum through the foramen magnum was seen in all cases (Figs 5, 6). The dens and lamina of C1 were prominent causing marked cord compression as well as obliteration of the cisterna magna CSF signal (Figs 5, 6). The middle and inner ear were normal in Cubs B–D. An incidental cyst-like lesion was visible in the left olfactory lobe in Cub A. Paramagnetic contrast administration did not result in any additional abnormalities being detected.

The various structures measured and their ratios are presented in Table 1. The parietal and caudal basisphenoid bones showed the least change but the affected cubs still had increased ratios compared to the vitreous humor on sagittal images indicating thickening of these bones compared to the control cub. The mean occipital bone ratios were 60% greater than the control cub indicating marked thickening (Figs 5, 6). The *tentorium cerebelli osseum* showed the most pronounced changes with mean thickness ratios being 115–168 % greater on the various imaging planes in affected cubs compared with the normal cub (Figs 5–7). The sum of cerebellar measurements had varying outcomes. The ventricles showed moderate enlargement with the average ventricular to cerebral ratio being nearly double that of the normal cub (Fig. 4). The minimum to maximum dorsoventral cervical spinal cord diameter ratios showed that in affected cubs the cord was compressed up to 40 % by enlarged surrounding osseous structures (Figs 5, 6).

The MRI of the normal cub showed normal conformation of the *tentorium cerebelli osseum* and associated bony structures of the cranial vault with no compression of the cerebellum and cranial spinal cord. The various measurements are given in Table 1.

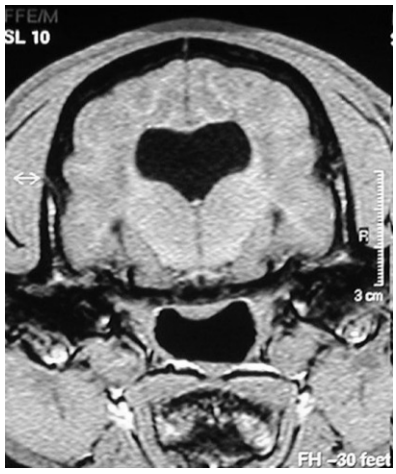

Fig. 4: **Transverse T1 weighted brain image of affected Cub A at the level of the interthalamic adhesion. Note the enlarged lateral ventricles. Lateral ventricle:cerebral ratio was 0.25. Ignore white double arrowhead on left of image.**

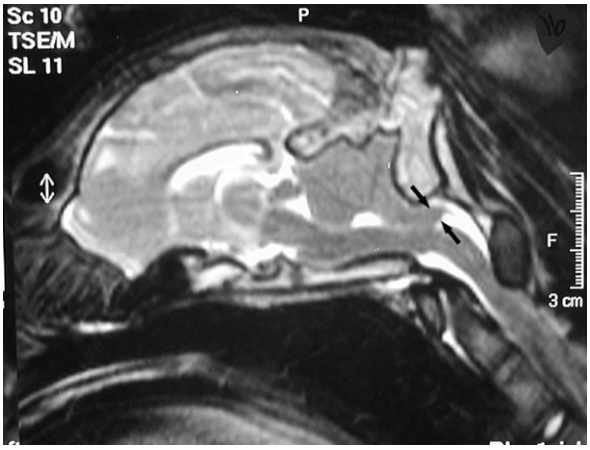

Fig. 5: **Sagittal midline T2 weighted brain image of affected Cub B. Note the compression and malformation of the cerebellum by the thickened *tentorium cerebelli osseum* and occipital bones. Note the partial herniation of the *uvula vermis* of the cerebellum through the foramen magnum** (black arrows)**. There is mild distension of the third ventricle and prominent communication between the lateral ventricles. The spinal cord is compressed by a grossly enlarged lamina of C1. The 4th ventricle is also focally dilated. Ignore white double arrowhead on left of image.**

The follow up MRI examination of Cub A 6 months later, after complete clinical recovery, showed the ventricular system still to be dilated but to a lesser extent than previously. The 3rd and 4th ventricles were no longer compressed. The *tentorium cerebelli osseum* was reduced in thickness (Table 1) with concomitant

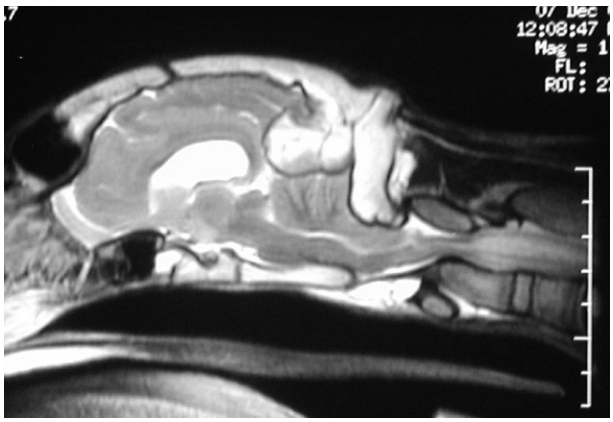

Fig. 6: **Sagittal midline T2 weighted brain image of affected Cub D. Note the compression and malformation of the cerebellum by the thickened *tentorium cerebelli osseum* and occipital bones. There is partial herniation of the *uvula vermis* of the cerebellum through the foramen magnum, prominent communication between the lateral ventricles and the spinal cord is compressed ventrally by the dens.**

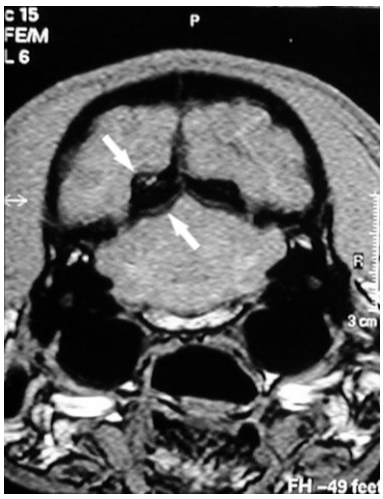

Fig. 7: **Transverse T1 weighted brain image of affected Cub A at the level of the *tentorium cerebelli osseum* which are markedly thickened** (white arrows)**. Ignore white double arrowhead on left of image.**

reduction in cerebellar compression. Most of the ratios showed an improvement.

After the diagnosis of suspected hypovitaminosis A was made using MRI, all the affected zoo cubs, their littermates and an unrelated litter consisting of 2 cubs which had begun to show mild head tilt and circling behaviour (total 7 cubs) were started on a course of Vitamin A (Vitamin A and E, Kyron Laboratories) treatment. A dose of 2000 IU/kg was administered by remote injection technique weekly for 4 weeks and then every 2 weeks for a further 4 doses. All cubs started showing some improvement within 2 weeks and all clinical signs had resolved after 3 months. Nutrition of the cubs was reviewed and whole carcass feeding, offal and commercial carnivore food was added to the diet. No further cases of hypovitaminosis A were diagnosed in the zoo following this dietary modification in the following 18 months up to the time of writing this article. Cub D was treated similarly and at the time of going to press was improving clinically.

DISCUSSION

Wild carnivores consume the majority of a carcass, including viscera, intestines and bones. In captivity animals are often fed a diet consisting solely of lean red meat. This predisposes the animals to various vitamin and mineral deficiencies, as these micronutrients are not found in muscle. Pure meat diets may result in nutritional secondary hyperparathyroidism or hypovitaminosis A.

Nutritional secondary hyperparathyroidism has been reported in lion[4,8] and tiger cubs[7]. This condition is caused by diets low in calcium and high in phosphorous, with accompanying deficiency in Vitamin D and typically results in poorly mineralised bones with the osteopenia resulting in secondary fractures and double cortical lines.

Hypovitaminosis A has been reported in lions on a number of occasions[1,2,6], but has not been reported in other large felids or the domestic cat. Domestic kittens experimentally fed a diet deficient in vitamin A failed to develop the clinical signs or lesions described in lions, but did develop obvious squamous metaplasia of the epithelia of the conjunctiva, trachea, salivary ducts and uterus[3]. Similar clinical signs to these lions were seen in domestic puppies with experimentally induced Vitamin A deficiency[5].

The cases described in this study did not have the diagnosis confirmed by blood or liver analyses, but the distinctive bony changes with the resultant compression of associated intracranial structures seen on MRI correlated very well with the described macroscopical pathological findings[2]. Additionally, the clinical signs and rapid response to treatment further supported the diagnosis. Magnetic resonance imaging clearly demonstrated the pathology typically associated with this condition. Measurement errors could have occurred as result of measurements being made manually on the small laser printed images. Accuracy will be enhanced if measurements are made directly on the computer screen at the time of the examination. The maximum diameter of structures may also have been slightly under measured due to slice intervals of up to 2 mm. Utilising the maximum diameter of the unaffected vitreous humor as a normal value to calculate ratios to accommodate the effect that varying ages and sizes may have had on measurements appears to have worked well. However, enlargement of the osseous orbit cannot be ruled out in the affected lions which could have resulted in a smaller vitreous humor. In the 4 affected cubs the *tentorium cerebelli osseum* and associated cranial bones were markedly thickened, with some more than 100 % thicker than those measured in the normal cub (Table 1). The recovered cub also had a marked improvement in the various ratios. The various measurements and ratios presented must, however, be interpreted with some caution as only a single cub acted as a control.

Compression of the intracranial structures by the thickened cranial bones resulted in loss of sulci visibility and compression of the 3rd and 4th ventricles. The latter resulted in mild to moderate secondary hydrocephalus of the lateral ventricles in all 4 cubs. The prominent dens caused cord compression, which may have contributed to the clinical signs. Vascular lesions are thought to play a major role in the pathogenesis of the condition, with the increased intracranial pressure leading to occlusion of blood flow and haemorrhage with secondary perivascular infiltration by mononuclear cells[2]. The vascular changes may also contribute to the clinical signs.

Hypovitaminosis A, causing the syndrome described here, has only been reported in lions under 1 year of age and usually between 5 and 9 months. It is during this period that the animals are undergoing rapid growth such that the skeletal changes are most severe and malformations occur. The changes in the bones are believed to be due to abnormal periosteal metabolism, resulting in an increased bone production[2]. This is thought to be due to failure of differentiation of the mesenchymal cell from osteoblast to osteoclast[2]. Mandibular thickening has also been described[2], but was not specifically evaluated in this study.

Hypovitaminosis A in adult animals causes reproductive infertility, congenital defects in offspring and respiratory disease, which is most likely due to squamous metaplasia of columnar and cuboidal epithelial tissues[2].

In all previous reports, vitamin A deficiency was diagnosed on *post mortem* examination, with confirmation by vitamin A analysis of liver tissue. Magnetic resonance imaging, although more expensive and requiring anaesthesia, clearly illustrates in a non-invasive manner the distinctive pathology seen in hypovitaminosis A. The authors recommend T1- and T2-weighted spin echo sequences be made in sagittal (from eye to C2) and transverse (olfactory lobe to C2) planes and making the following measurements as described: vitreous humor diameter, *tentorium cerebelli osseum,* occipital bone

Table 1: **Various measurements and ratios made from MRI images of 4 lion cubs with suspected hypovitaminosis A.**

Parameters measured in mm See text for details		Cub A		Cub A follow up		Cub B		Cub C		Cub D		Cubs A–D mean measurement		Cub E (normal)	
		Av.[a]	Ratio[b]	Av.	Ratio	Av.	Ratio	Av.	Ratio	Av.	Ratio	Av.	Ratio	Av.	Ratio
Parasagittal images of *tentorium*	Left	12.46	0.50	9.99	0.35	11.51	0.39	15.74	0.50	8.86	0.33	12.14	0.43	6.43	0.20
	Right	10.29	0.41	10.23	0.36	11.81	0.40	16.85	0.53	16.34	0.62	13.8	0.49	6.55	0.20
Transverse images of *tentorium*	Left	12.69	0.51	7.53	0.26	11.30	0.38	11.61	0.37	11.99	0.45	11.9	0.43	5.09	0.16
	Right	10.01	0.40	8.61	0.30	10.90	0.37	12.27	0.39	12.09	0.46	11.32	0.41	5.17	0.16
Midline sagittal parietal bone		6.38	0.26	8.04	0.28	6.40	0.22	12.95	0.41	7.48	0.28	8.30	0.29	7.26	0.22
Midline sagittal caudal basisphenoid bone		13.33	0.53	5.87	0.20	7.77	0.26	12.70	0.40	7.48	0.28	10.32	0.37	9.17	0.28
Midline transverse basisphenoid bone		6.50	0.26	7.75	0.27	6.67	0.22	10.22	0.32	6.15	0.23	7.39	0.26	9.35	0.29
Midline sagittal occipital bone		13.5	0.54	14.37	0.50	13.54	0.46	17.65	0.56	12.06	0.46	14.19	0.51	10.48	0.32
Transverse latero–lateral diameter of cerebellum	(A)	49.61	1.99	53.67	1.86	48.45	1.63	49.64	1.57	48.98	1.85	49.17	1.76	52.5	1.62
Transverse DV diameter cerebellum and brainstem	(B)	33.28	1.33	36.56	1.27	29.61	1.00	29.13	0.92	31.36	1.18	30.85	1.11	35.23	1.08
Sum of A and B above		82.89	3.32	90.23	3.13	78.06	2.63	78.77	2.48	80.34	3.04	80.02	2.87	87.74	2.70
Midline sagittal minimum DV cord diameter	(A)	6.31	0.25	5.65	0.20	5.56	0.19	5.85	0.18	5.78	0.22	5.88	0.21	5.60	0.17
Midline sagittal maximum DV cord diameter	(B)	11.31	0.45	6.00	0.21	10.50	0.35	6.86	0.22	14.23	0.54	10.73	0.39	5.72	0.18
Ratio of A:B above		0.56	–	0.94	–	0.53	–	0.85	–	0.41	–	0.59	–	0.98	–
Transverse maximum DV diameter of lateral ventricles	Left	13.8	0.55	14.89	0.52	7.87	0.26	7.54	0.24	9.18	0.35	9.59	0.35	4.5	0.14
	Right	13.8	0.55	14.89	0.52	8.27	0.28	6.67	0.21	9.18	0.35	9.48	0.35	4.52	0.14
Transverse maximum DV cerebrum diameter		54.52	2.18	66.81	2.32	49.20	1.66	48.12	1.52	50.61	1.91	50.61	1.82	46.29	1.42
Ratio lateral ventricle to cerebrum	Left	–	0.25	–	0.22	–	0.16	–	0.16	–	0.18	–	0.19	–	0.10
	Right	–	0.25	–	0.22	–	0.17	–	0.14	–	0.18	–	0.19	–	0.10
Sagittal maximum diameter of vitreous humor	Left	25.24	–	28.63	–	29.70	–	31.70	–	26.75	–	–	–	32.50	–
	Right	24.67	–	28.97	–	29.70	–	31.70	–	26.18	–	–	–	32.50	–
Average of left and right vitreous humor diameters		24.96	–	28.80	–	29.70	–	31.70	–	26.47	–	–	–	32.50	–

[a]Average value of measurements made by 2 observers.
[b]Ratio of structure measured: average diameter of vitreous humor.

and cervical spinal cord. Abnormal values and ratios are highly suggestive for the diagnosis and allows for early treatment of the condition which to date has resulted in recovery of the patients.

ACKNOWLEDGEMENTS

We thank Drs N Keller and L Venter allowing us to use data from cub D for this article.

REFERENCES

1. Baker J R, Lyon D G 1977 Skull malformation and cerebellar herniation in captive African lion. *Veterinary Record* 10: 154–1560
2. Bartsch R C, Imes G D, Smit J P 1975 Vitamin A deficiency in the captive African lion cub. *Onderstepoort Journal of Veterinary Research* 42: 43–54
3. Gershoff S N, Andrus S B, Hegsted D M, Lentini E 1957 Vitamin A deficiency in cats. *Laboratory Investigation* 6: 227–240
4. Herz V, Kirberger R M 2004 Nutritional secondary hyperparathyroidism in a white lion cub (*Panthera leo*), with concomitant radiographic double cortical line. *Journal of South African Veterinary Association* 75: 49–53
5. Mellanby E 1941 Skeletal changes affecting the nervous system produced in dogs by diets deficient in Vitamin A. *Journal of Physiology* 99: 467–486
6. O'Sullivan B M, Mayo F D, Hartley W J 1977 Neurological lesions in young captive lions associated with vitamin A deficiency. *Australian Veterinary Journal* 53: 187–189
7. Slusher R, Bistner S I, Kircher C 1965 Nutritional secondary hyperparathyroidism in a tiger. *Journal of the American Veterinary Medical Association* 147: 1109–1115
8. Van Rensburg I B J, Lowry M H 1988 Nutritional secondary hyperparathyroidism in a lion (*Panthera leo*) cub. *Journal of the South African Veterinary Association* 59: 83–87